Laser modes with helical wave fronts

M. Harris,* C. A. Hill, P. R. Tapster, and J. M. Vaughan
Defence Research Agency Malvern, St. Andrews Road, Malvern, Worcestershire WR14 3PS, United Kingdom
(Received 17 September 1993)

We report the operation of an argon-ion laser in pure (single-frequency) "doughnut" modes of order $m=1$, 2, and 3. The phase discontinuity at the center of these modes leads to striking two-beam interference patterns that clearly demonstrate the existence of a helical cophasal surface (wave front). The doughnut mode with $m=1$ (usually called TEM_{01}^{*}) displays a forking interference fringe pattern characteristic of a pure single helix. The $m=2$ mode shows a pattern with four extra prongs, establishing that the cophasal surface is a two-start or double helix; the $m=3$ mode is a triple helix with a six-extra-pronged pattern. Each pure doughnut mode is shown to have two possible states corresponding to output wave fronts of opposite helicity.

PACS number(s): 42.60.−v

It has long been appreciated that a light beam can possess a helical cophasal surface (wave front). This was first demonstrated in 1979 for a TEM_{01}^{*} laser doughnut mode from the analysis of interference patterns [1]. This helical form, implicit in previous analyses of cavity eigenfunctions, was examined by frequency measurements, computer modeling, and further interference experiments [2]. Similar phase discontinuities and optical vortices have been studied by several authors, uncovering a rich complexity of transverse-mode patterns in optical cavities and other areas of physics [3], and which can be related to earlier treatments [4] of dislocations in general wave trains. However, convincing experimental evidence of the helical properties of pure doughnut laser modes has so far proved elusive; although some interference fringe data have been obtained [see, for example, Fig. 4(b) of [5] for first-order and Fig. 7 of [6] for first- and second-order doughnuts], their rather poor visibility precludes an assessment of mode purity. In this paper, we report laser operation in pure doughnut modes of order $m=1$, 2, and 3, and use a two-beam interference technique to demonstrate clearly the existence of the helical wave front. Optical helical modes have angular-momentum properties of current interest [7] and also have potential for laser focusing of atoms [8].

Laser doughnut modes may be represented as a linear combination of Hermite-Gaussian or Laguerre-Gaussian beams. In many lasers, two or more of these components oscillate independently at different frequencies [1]. For the $m=1$ doughnut (usually labeled TEM_{01}^{*}) this implies that the wave front of the output light evolves back and forth between left-handed and right-handed helicity [1,2] on a time scale determined by the difference (beat) frequency of the two constituent modes. The mode frequency splitting (nondegeneracy) arises from the astigmatism that elements such as Brewster windows introduce into the cavity [9]. This splitting is typically rather small (of order 1 MHz). However, for a laser with a wide gain bandwidth, the modes usually choose to lase with different longitudinal mode number [10] and are therefore split by approximately a multiple of $\Delta=c/2L$ [1]. Here, we describe a technique that achieves laser operation in *degenerate* (single-frequency) doughnut modes of order 1, 2, and 3. Each of these modes has a fixed helicity. An optical arrangement for achieving a single-frequency helix was described in [2]; such modes have also been produced in lasers with narrow gain bandwidth (i.e., less than Δ) [11], with mode converters [12], and by holographic techniques [6].

In our experiments, we have used a modified Lexel Model 95 double-ended argon-ion laser, with a temperature-controlled intracavity étalon to ensure a single-frequency TEM_{00} mode under normal operating conditions [13]. The laser cavity length L is approximately 1 m, giving a longitudinal-mode spacing Δ of 156.02 MHz. The mirrors have radii of curvature of 4.8 and 3.9 m, and their transmissivities are each of order 5%. The bore of the discharge has a diameter of 4 mm. The properties of the subthreshold transverse modes of the basic laser have previously been studied in detail using a new experimental technique reported elsewhere [14]. Our recipe for achieving a degenerate doughnut mode is similar to that used in [11] and consists first of obtaining the nondegenerate doughnut by inserting a small circular absorber into the cavity, centered on axis, in order to suppress the TEM_{00} mode. The output is then a superposition of modes at different frequencies, which are tuned to achieve single-frequency operation. Throughout all our experiments the beam remains *linearly* polarized. The light output is monitored in several ways (Fig. 1). Firstly, its gross shape is monitored by beam expansion and projection onto a screen. Secondly, a direct measurement of the light spectrum is made with a confocal Fabry-Pérot étalon. Thirdly, the beat spectrum of light is obtained by spectral analysis of the photocurrent from a detector. Finally, interference patterns are formed by mixing the output beam with its mirror image (Fig. 2); these will be described later.

*FAX: 44 684 896270.

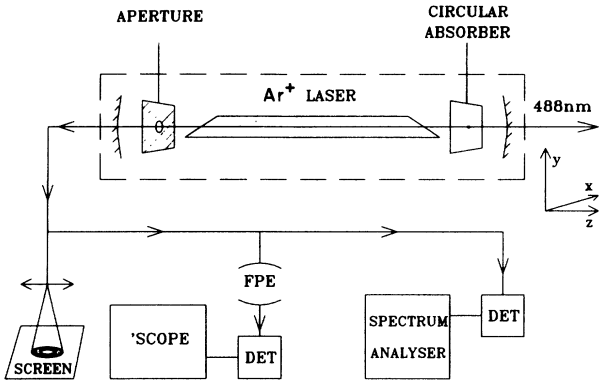

FIG. 1. The experimental setup. The aperture and circular absorber define the spatial mode of the laser, and the output spectrum and spatial properties are then monitored in several ways, as explained in the text. FPE—confocal Fabry-Pérot étalon. DET—detector.

We now provide a more detailed description of the procedure used to obtain helical laser modes. An array of small circular absorbers of diameter ranging from 50 to 500 μm, deposited onto a glass plate, is mounted on an X-Y translation stage (Fig. 1). This is inserted into the cavity and positioned so as to maximize the power of the desired doughnut mode. The circular aperture (Fig. 1) is also mounted on an X-Y stage; the mode order is selected by choosing an appropriate absorber diameter and aperture size. Normally, the laser output shows two spectral components of the nondegenerate doughnut mode. For the first-order doughnut these are the TEM_{01} and TEM_{10} transverse laser modes, and they give rise to a strong beat signal close to the longitudinal-mode spacing. The frequency of this beat is then tuned by applying an astigmatic perturbation to the cavity by translating either the intracavity absorber or aperture. The aim is to tune the beat frequency as close as possible to the exact longitudinal-mode spacing ($\Delta = 156.02$ MHz) because this indicates that the TEM_{01} and TEM_{10} modes are approaching degeneracy, thus creating favorable conditions for frequency locking. When the beat gets within about 0.5 MHz of Δ, the beat suddenly disappears, and the étalon confirms that the laser is now running on a single-frequency. This cooperative frequency locking of the constituent modes is closely related to the "lock-up" behavior of counterpropagating beams in a laser gyro [15]. The first-order degenerate doughnut mode can be expressed as the sum of the pair of two-lobe (TEM_{01} and TEM_{10}) modes, phase locked in quadrature. This relative phase permits the most efficient use of the laser gain medium [11]. The doughnut modes appear to be quite stable, operating over a wide range of laser powers up to 30 mW.

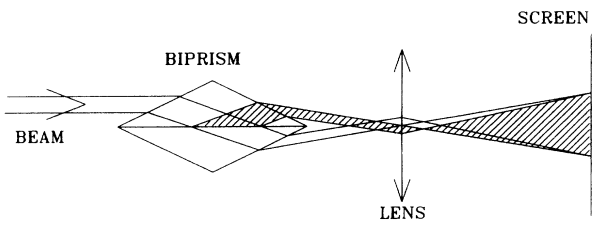

FIG. 2. The optical arrangement for interference of the beam with its mirror image. If the input beam enters the other port of the beamsplitter, then the interference pattern becomes the "negative" of those in Fig. 3.

The helical character of each doughnut mode is clearly demonstrated by observing the interference fringe patterns when the beam intersects its own mirror image (which has opposite helicity) at a small angle. Figure 2 demonstrates how this was achieved with a biprism beam splitter [1,2]. This yields fringe visibility greatly superior to that of the conventional methods involving either interferences of displaced beams [5] or the superposition of a reference plane-wave laser beam [6], since in our case the beams have equal intensity throughout the pattern. Alternatively, the fringe patterns may be formed by interfering the laser beams from front and back ends of the laser, as these must already possess opposite helicities (any reflection causes a change of handedness). Photographic examples of the fringe patterns for modes of order $m=1$ are displayed in Fig. 3. The most striking feature of these patterns is the fringe splitting or "forking" arising from the phase discontinuity at the center of the mode. For the TEM_{01}^{*} mode [Figs. 3(b) and 3(c)], this gives rise to two extra dark fringes on one side of the pattern, whereas the second-order mode [Fig. 4(a)] has four and the third-order [Fig. 4(b)] has six. The extra fringes come about because the wave fronts of two opposite-sign helices intersect at different angles on either side of the pattern: the position of the fringes on one side or the other allows us to determine the handedness of the output beam. It is simple to demonstrate that the helical modes each have two possible states, corresponding to opposite handedness, because a change of handedness leads to an inversion of the forking fringe pattern [Fig. 3(c)]. Preliminary statistics indicate that when a degenerate doughnut mode is allowed to build up out of spontaneous noise, there is roughly a 50% probability of creating either handedness: the pattern seems equally likely to be "heads" or "tails."

It is straightforward to derive the theoretical form of the interference patterns. The TEM_{01}^{*}-mode electric field is given approximately [16] by

$$E = E_0 r e^{-r^2/2a^2} e^{\pm i\theta} , \tag{1}$$

where the $+$ or $-$ defines the handedness of the helix. E_0 and a are constants determining the intensity and diameter of the beam. For the mode of order m, the field becomes

$$E = E_0 r^m e^{-r^2/2a^2} e^{\pm im\theta} . \tag{2}$$

In our experiments, such a helical mode intersects its own mirror image at a small angle on a screen (Fig. 2). Thus, the combined field for TEM_{01}^{*} at the screen is given by

$$E = (e^{i\alpha x} e^{\pm i\theta} + e^{-i\alpha x} e^{\mp i\theta}) E_0 r e^{-r^2/2a^2} , \tag{3}$$

where α represents an arbitrary angle of intersection, in

this case the fringes run roughly perpendicular to the x axis. The resulting interference pattern is given by the intensity distribution for the single beam $[I_0(r)]$, multiplied by the contribution from the phase part; this is the square modulus of Eq. (3):

$$I = I_0(r)\cos^2[\alpha x \pm \theta]$$
$$= E_0^2[x\cos(\alpha x) \pm y\sin(\alpha x)]^2 e^{-(x^2+y^2)/a^2}. \quad (4)$$

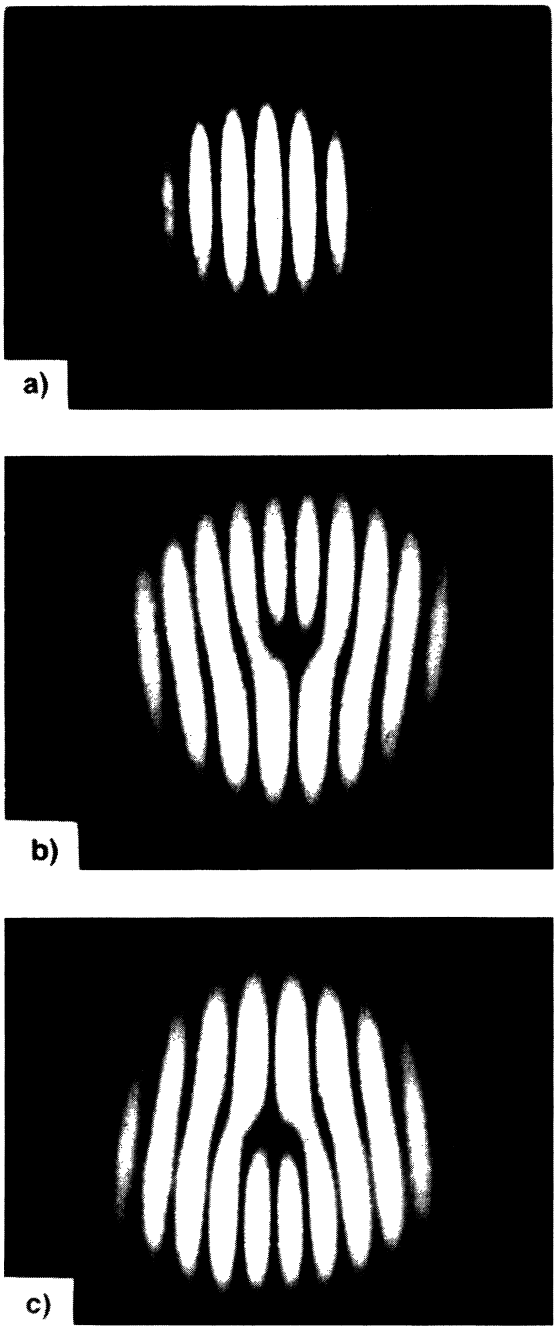

FIG. 3. Photographs of experimental interference fringe patterns: (a) Normal operation (TEM_{00} mode); (b) Lowest-order doughnut (TEM_{01}^*) mode; (c) TEM_{01}^* mode [opposite helicity to (b)].

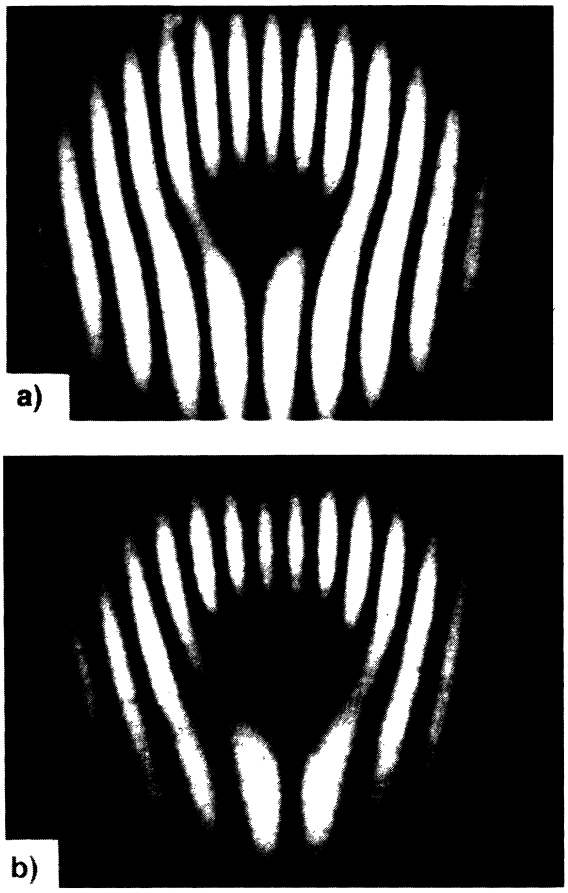

FIG. 4. Experimental interference patterns for (a) second- and (b) third-order doughnut modes.

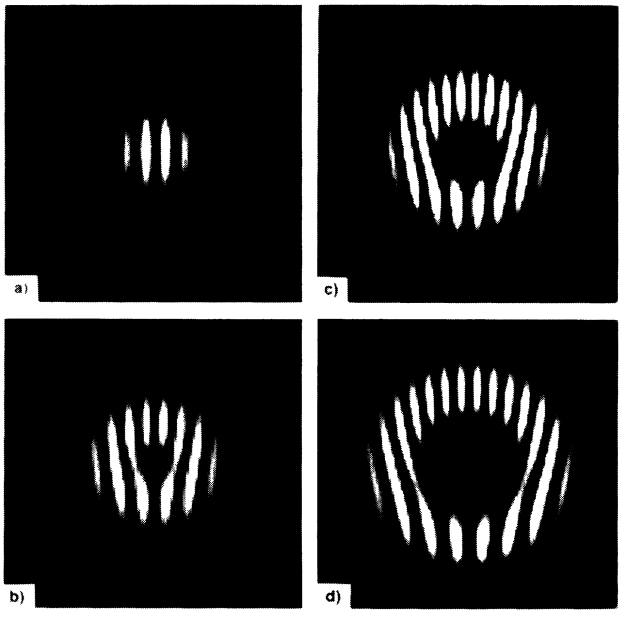

FIG. 5. Computer-generated theoretical density plots of the interference patterns shown in Figs. 3 and 4. Lighter shading indicates higher intensity. (a) TEM_{00} mode. (b) First-order doughnut mode (TEM_{01}^*). (c) Second-order doughnut. (d) Third order.

For the higher-order modes, the corresponding intensity pattern is given by

$$I = I_0(r)\cos^2[\alpha x \pm m\theta] \ . \tag{5}$$

The theoretical patterns are displayed in Fig. 5 in the form of a density plot where lighter shading corresponds to higher intensity. The plots in Fig. 5 demonstrate excellent agreement with the experimental data of Figs. 3 and 4. The results confirm the implication of Eq. (1) that the wave front of the TEM_{01}^{*} mode consists of a simple helix of pitch λ (sometimes referred to as an *optical vortex* with a *charge* of 1). However, the second-order mode wave front must consist of two helices, each of pitch 2λ (i.e., with a charge of 2), displaced longitudinally by λ. This double or *two-start* helix is clearly necessary for consistency with the beam's frequency. Likewise, the $m=3$ mode wave front is a triple or three-start helix; each has pitch 3λ, again displaced longitudinally by λ.

In summary, we have obtained pure laser doughnut modes of order 1, 2, and 3. The laser output has been used to create two-beam interference patterns that unequivocally demonstrate the helical nature of the wave front. The higher-order doughnut modes possess a helical wave front of increased pitch; this implies that the wave front must have a multistart character.

We wish to acknowledge useful discussions with D. V. Willetts, L. Allen, R. Loudon, T. J. Shepherd, and E. Jakeman.

[1] J. M. Vaughan and D. V. Willetts, Opt. Commun. **30**, 263 (1979).

[2] J. M. Vaughan and D. V. Willetts, J. Opt. Soc. Am. **73**, 1018 (1983).

[3] See, for example, the following and references therein: P. N. Pusey, J. M. Vaughan, and D. V. Willetts, J. Opt. Soc. Am. **73**, 1012 (1983); J. R. Tredicce, E. J. Quel, A. M. Ghazzawi, C. Green, M. A. Pernigo, L. M. Narducci, and L. A. Lugiato, Phys. Rev. Lett. **62**, 1274 (1989); P. Coullet, L. Gil, and F. Rocca, Opt. Commun. **73**, 403 (1989); C. Tamm and C. O. Weiss, J. Opt. Soc. Am. B **7**, 1034 (1990); M. Brambilla, F. Battipede, L. A. Lugiato, V. Penna, F. Prati, C. Tamm, and C. O. Weiss, Phys. Rev. A **43**, 5090 (1991); F. T. Arecchi, G. Giacomelli, P. L. Ramazza, and S. Residori, Phys. Rev. Lett. **67**, 3749 (1991); K. Staliunas, Opt. Commun. **90**, 123 (1992); D. Hennequin, C. Lepers, E. Louvergneaux, D. Dangoisse, and P. Glorieux, *ibid.* **93**, 318 (1992); V. I. Kruglov, Y. A. Logvin, and V. M. Volkov, J. Mod. Opt. **39**, 2277 (1992); G. Indebetouw, *ibid.* **40**, 73 (1993).

[4] J. F. Nye and M. V. Berry, Proc. R. Soc. London Ser. **336**, 165 (1974).

[5] A. G. White, C. P. Smith, N. R. Heckenburg, H. Rubinsztein-Dunlop, R. McDuff, C. O. Weiss, and C. Tamm, J. Mod. Opt. **38**, 2531 (1991).

[6] N. R. Heckenburg, R. McDuff, C. P. Smith, H. Rubinsztein-Dunlop, and M. J. Wegener, Opt. Quantum Electron. **24**, S951 (1992).

[7] L. Allen, M. W. Beijersbergen, R. J. C. Spreeuw, and J. P. Woerdman, Phys. Rev. A **45**, 8185 (1992).

[8] J. J. McClelland and M. R. Scheinfein, J. Opt. Soc. Am. B **8**, 1974 (1991).

[9] A. E. Siegman, *Lasers* (University Science, Mill Valley, CA, 1986), Chap. 17, p. 689.

[10] The preference of the laser for oscillation on two modes widely spaced in frequency reflects the role of population pulsations in mode competition and will be the subject of a later paper.

[11] C. Tamm, Phys. Rev. A **38**, 5960 (1988).

[12] M. W. Beijersbergen, L. Allen, H. E. L. O. van der Veen, and J. P. Woerdman, Opt. Commun. **96**, 123 (1993).

[13] M. Harris, R. Loudon, G. L. Mander, and J. M. Vaughan, Phys. Rev. Lett. **67**, 1743 (1991).

[14] M. Harris, C. A. Hill, and J. M. Vaughan, Electron. Lett. **29**, 997 (1993).

[15] A. E. Siegman, *Lasers* (Ref. [9]), Chap. 29, p. 1162.

[16] For simplicity, we are ignoring here the perturbing effect of aperture and circular absorber on the resonator mode solutions.

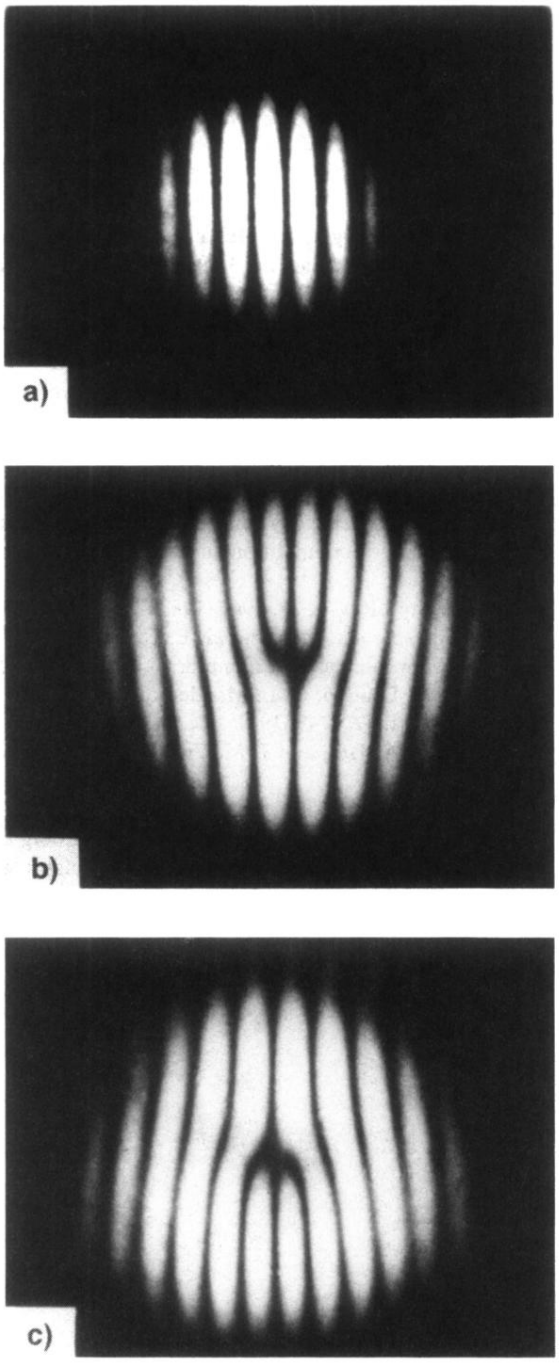

FIG. 3. Photographs of experimental interference fringe patterns: (a) Normal operation (TEM_{00} mode); (b) Lowest-order doughnut (TEM^{*}_{01}) mode; (c) TEM^{*}_{01} mode [opposite helicity to (b)].

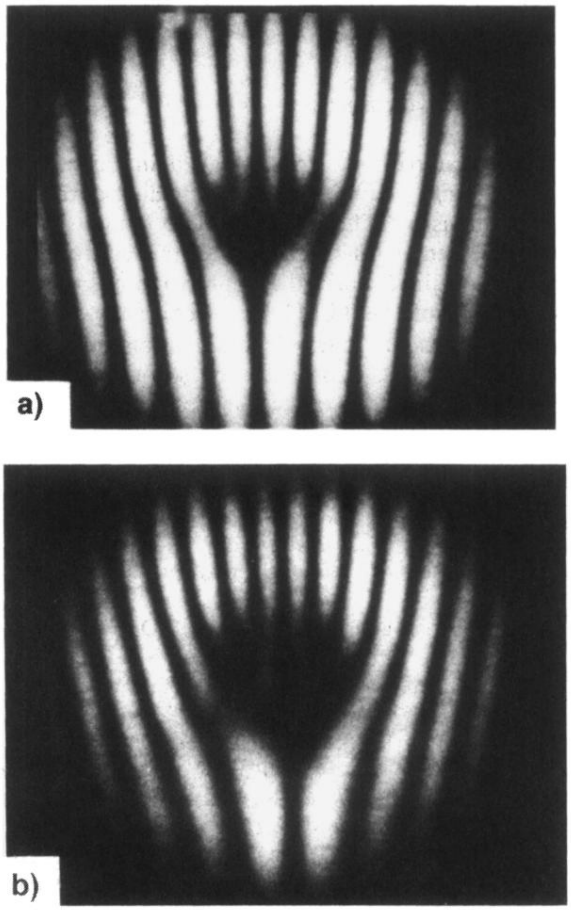

FIG. 4. Experimental interference patterns for (a) second- and (b) third-order doughnut modes.

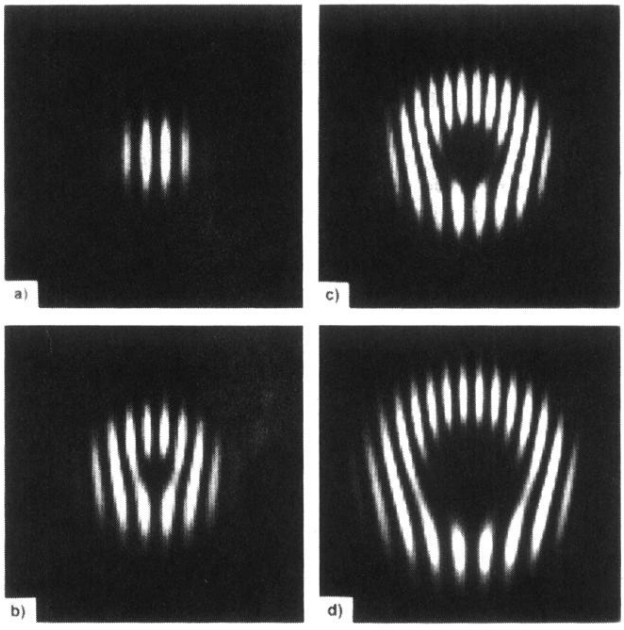

FIG. 5. Computer-generated theoretical density plots of the interference patterns shown in Figs. 3 and 4. Lighter shading indicates higher intensity. (a) TEM_{00} mode. (b) First-order doughnut mode (TEM_{01}^{*}). (c) Second-order doughnut. (d) Third order.